SOFIA/GREAT [CII] observations in nearby clouds near the lines of sight towards B0355+508 and B0212+735

Jürgen Stutzki
I. Physikalisches Institut, Universität zu Köln

SFB 956 (Coordinated Research Center 956)
“Conditions and Impact of Star Formation”
Sub-Project A4

Co-PI of GREAT/upGREAT Instrument on SOFIA

Overview

- Science context
- Proposal
- Observations
- Interpretation and analysis
- Summary

Overview

- **Science context**
- **Proposal**
- **Observations**
- **Interpretation and analysis**
- **Summary**

- **Science Context**
  - **CO-dark gas is a "hot topic" since the Herschel GOT C+ results**
  - **diffuse clouds**
    - **clouds in formation**
    - **not yet formed heavy molecules (carbon mostly not yet in CO)**
    - **studied e.g. by mm-wave absorption against Quasar background source (Lizt, Lucas, Pety papers)**
  - **a systematic study in CO (IRAM 30m) revealed (Liszt & Pety, 2012)**
    - **weak CO J=1-0**
    - **CO J=2-1/J=1-0 intensity ratio: low excitation temperature**
      - › **interpreted to be sub-thermally excited due to low density (as diffuse cloud should not be very cold)**
    - **small scale spatial variations in CO brightness**
      - › **Interpreted as chemical fluctuations, not cloud density structure**

A_V and CO maps (Liszt & Pety, 2012, A&A 541, A58)

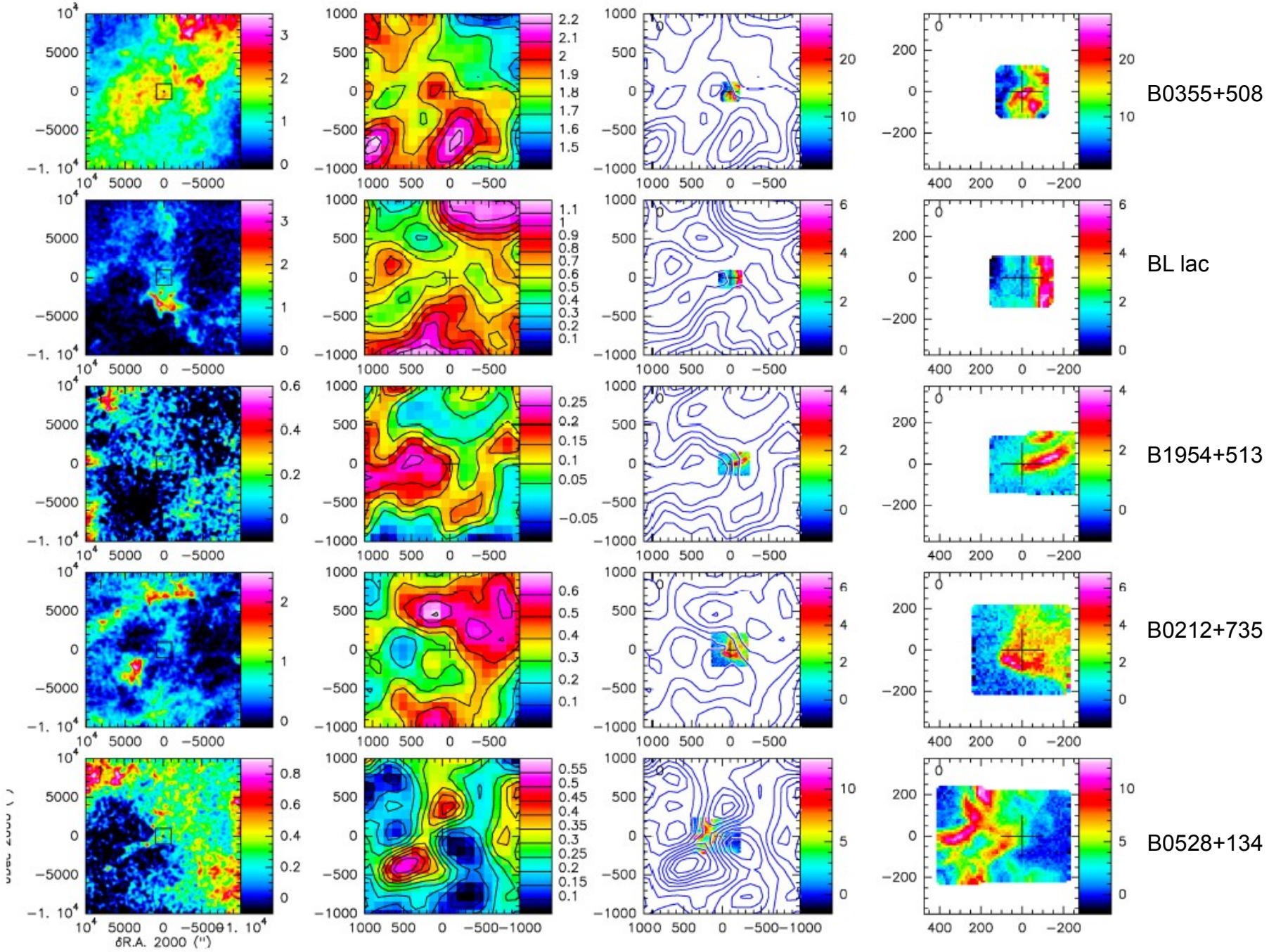

SOFIA/GREAT [CII] observations in nearby clouds near the lines of sight towards B0355+508 and B0212+735

- **Science Context (continued)**
  - **dominant coolant should be through [CII] 158 um**
    - **CO not abundant and only weakly excited**
    - **[OI] 63 um needs high temperature and high density**
  - **heating**
    - **average FUV field in the Milky Way**
    - **possibly turbulent dissipation**
    - **unavoidable: cosmic ray heating**
  - **relatively simple physics, hence good model predictions**

Overview

- Science context
- Proposal
- Observations
- Interpretation and analysis
- Summary

- **The Proposal Idea**
  - **if the above picture**
    - **diffuse clouds**
    - **chemical fluctuations cause CO spotiness**

    is correct, we would expect
    - **reasonably bright [CII] emission**
    - **anticorrelated with CO distribution**

  - **hence**
    - **pick selection of Quasar-background diffuse clouds that have been mapped in CO**
    - **do deep integrations in [CII] at CO peaks and voids**

    to check the above scenarios!

  - **Cycle-1 proposal, A-rated, observed 2013/2014**
  - **PI: Christian Glück, PhD student in Cologne**
    (involved in failed STO [CII] survey,
    M33 HIFI-Herschel [CII] observations)

predicted [CII] intensity for diffuse cloud scenario

- **balance between heating and cooling**
  - **heating: photoelectric, Habing FUV field** G_0
    - **for low density** $n_H \leq 3 \times 10^3\,\mathrm{cm}^{-3}$
    - **temperature** $T \leq 100\,\mathrm{K}$

$$\Gamma_{pe} = 5 \times 10^{-26}\, G_0\, \mathrm{erg\,s^{-1}\,(H-atom)^{-1}}$$ Bakes & Tielens, 2010,ApJ 427, 822

    - **note: 17 times stronger than penetrating cosmic ray heating**

$$\Gamma_{cr} \approx 3 \times 10^{-27}\, \mathrm{erg\,s^{-1}\,(H-atom)^{-1}}$$

    - **other heating even less: turbulent dissipation (Falgarone et al. 2010), H_2 formation (Liszt & Lucas, 1996), ...**

  - **cooling: via [CII] 158 µm**
    - **cooling function**

$$I([CII])\left[\frac{\mathrm{K}}{\mathrm{km\,s}}\right] = \frac{1}{4\pi}\frac{c^3}{2\,k_B\,\nu^3}\,10^{-5}\,\Gamma_{pe}\,G_0\,N(H)$$

predicted [CII] line integrated intensities around 1-5 K km/s

proposal predictions

1-5 K km/s

(1)	(2)	(3)	(4)	(5)	(6)	(7)	(8)	(9)
Source	ra	dec	N_{tot} (H)	CII line int.	linew.	# of res. el. per linewi.	S/N	tot. est. time per point
	(J2000)	(J2000)	10^{21} cm^{-3}	10^{-6} $\frac{erg}{cm^2\ s\ sr}$	$\frac{km}{sec}$			sec
B1954+513	19:55:42.7	51:31:48.5	2.27	4.80	0.8	5	5	825
B0528+134	05:30:46.4	13:31:55.1	4.67	9.87	3.3	5	5	1005
BL Lac	22:02:43.2	42:16:39.9	2.73	5.77	1.4	6	4	958
B0212+735	02:17:30.8	73:49:32.6	6.93	14.64	2.0	6	5	956
B0355+508	03:59:29.7	50:57:50.1	5.32	11.24	3.2	5	6	900

Table 1: The table lists the proposed sources with their positions, total hydrogen column density, expected [CII] integrated line intensity, linewidth, number of resolution elements per linewidth, the signal to noise ratio and the total estimated time per point.
The parameters '# of resolution per linewidth' and 'signal to noise' have been fine tuned for all sources to get a total time per point of ~1000 sec.
B0355+508 has a high column density which arises from a high number of individual clouds with individual velocities. To get a realistic time estimate the column density was downscaled.

Overview

- Science context
- Proposal
- Observations
- Interpretation and analysis
- Summary

Observations

(1)	(2)	(3)	(4)	(5)	(6)	(7)	(8)	(9)
Source	ra	dec	N_{tot} (H)	CII line int.	linew.	# of res. el. per linewi.	S/N	tot. est. time per point
	(J2000)	(J2000)	10^{21} cm^{-3}	10^{-6} $\frac{erg}{cm^2\ s\ sr}$	$\frac{km}{sec}$			sec
B1954+513	19:55:42.7	51:31:48.5	2.27	4.80	0.8	5	5	825
B0528+134	05:30:46.4	13:31:55.1	4.67	9.87	3.3	5	5	1005
BL Lac	22:02:43.2	42:16:39.9	2.73	5.77	1.4	6	4	958
B0212+735	02:17:30.8	73:49:32.6	6.93	14.64	2.0	6	5	956
B0355+508	03:59:29.7	50:57:50.1	5.32	11.24	3.2	5	6	900

Table 1: The table lists the proposed sources with their positions, total hydrogen column density, expected [CII] integrated line intensity, linewidth, number of resolution elements per linewidth, the signal to noise ratio and the total estimated time per point.
The parameters '# of resolution per linewidth' and 'signal to noise' have been fine tuned for all sources to get a total time per point of ~1000 sec.
B0355+508 has a high column density which arises from a high number of individual clouds with individual velocities. To get a realistic time estimate the column density was downscaled.

- November 2013, February 2014
- GREAT L2 channel
- total power ON-OFF, OFF about 10-12 arcmins away

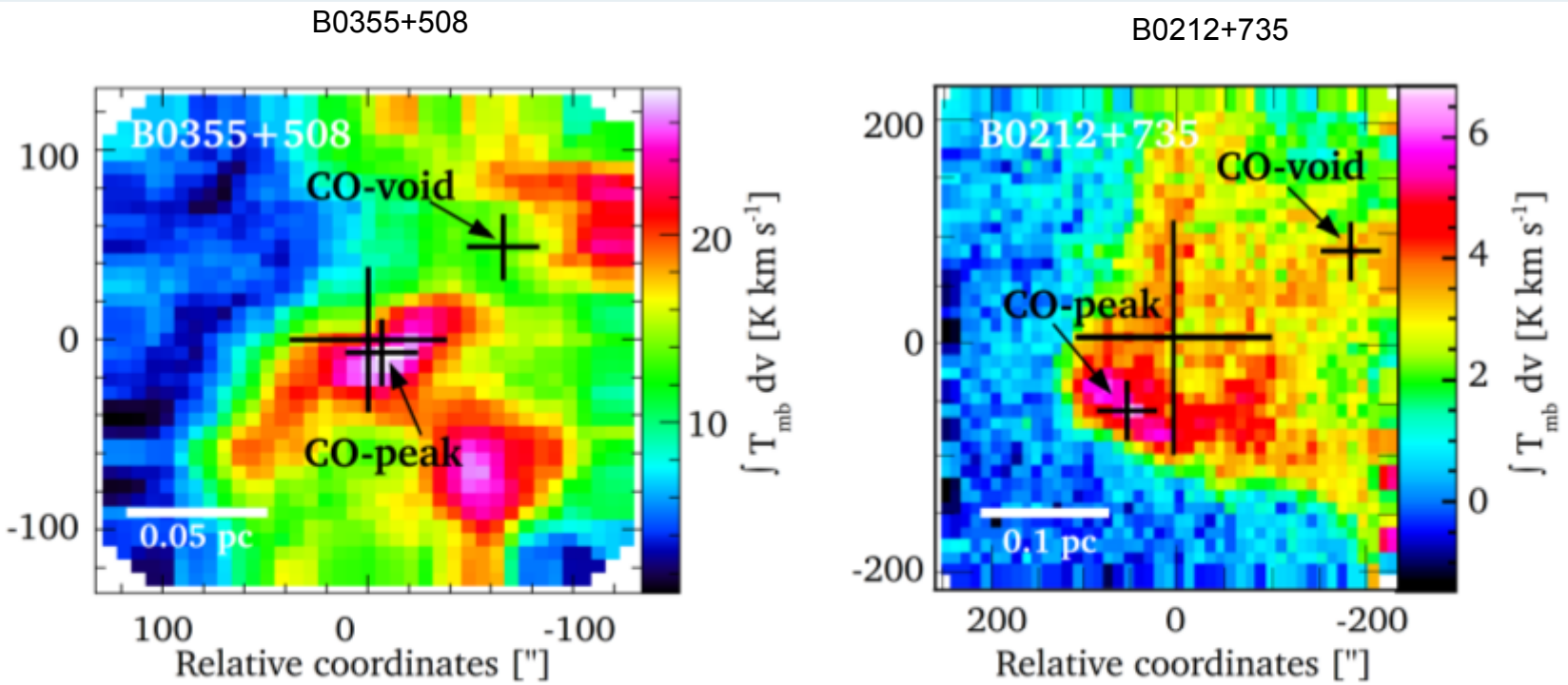

Fig. 1. Integrated CO (J=1–0) emission around B0355+508 (Liszt & Pety 2012) and B0212+735 (Pety & Liszt in prep.). Small crosses mark the positions observed in [C II]. The large cross in the middle marks the lines of sight towards B0355+508 and B0212+735. The length of the white bar corresponds to 0.05 pc in B0355+508 and 0.1 pc in B0212+735 for an assumed source distances of 150pc (Liszt & Pety 2012).

selected for minimal A_V and/or IRAS 100 µm

Table 1. Position of the [C II] observations

Source	(1) Centre position Ra (J2000)	Dec (J2000)	(2) CO-peak rel. offsets Ra (″)	Dec (″)	(3) CO-void rel. offsets Ra (″)	Dec (″)	(4) Off-position rel. offsets Ra (″)	Dec (″)
B0355+508	03:59:29.73	50:57:50.1	-7	-6	-57	+38	+190	+430
B0212+735	02:17:30.81	73:49:32.6	+47	-64	-187	+86	+607	+33

Notes. Coordinates (J2000) of B0355+508 and B0212+735 (1). Rows (2) and (3) show the relative offsets to the CO-peak and CO-void. The relative offsets of the off-positions are listed in row (4). Images of the integrated CO emission of the sources are shown in Fig. 1.

in press

Astronomy & Astrophysics manuscript no. 26454_ap_CG_print
July 11, 2016

SOFIA/GREAT [C II] observations in nearby clouds near the lines of sight towards B0355+508 and B0212+735

C. B. Glück[1], J.Stutzki[1], M. Röllig[1], E.T. Chambers[2, 1], and C. Risacher[3]

[1] I. Physikalisches Institut Universität zu Köln, Zülpicher Straße 77, 50937 Köln
e-mail: glueck@ph1.uni-koeln.de
e-mail: stutzki@ph1.uni-koeln.de
e-mail: roellig@ph1.uni-koeln.de
[2] SOFIA-USRA, NASA Ames Research Center, Mail Stop 232-12, Moffett Field, CA 94035-0001, USA
e-mail: echambers@sofia.usra.edu
[3] Max-Planck-Institut für Radioastronomie, Auf dem Hügel 69, 53121 Bonn, Germany
e-mail: crisache@mpifr-bonn.mpg.de

observational results

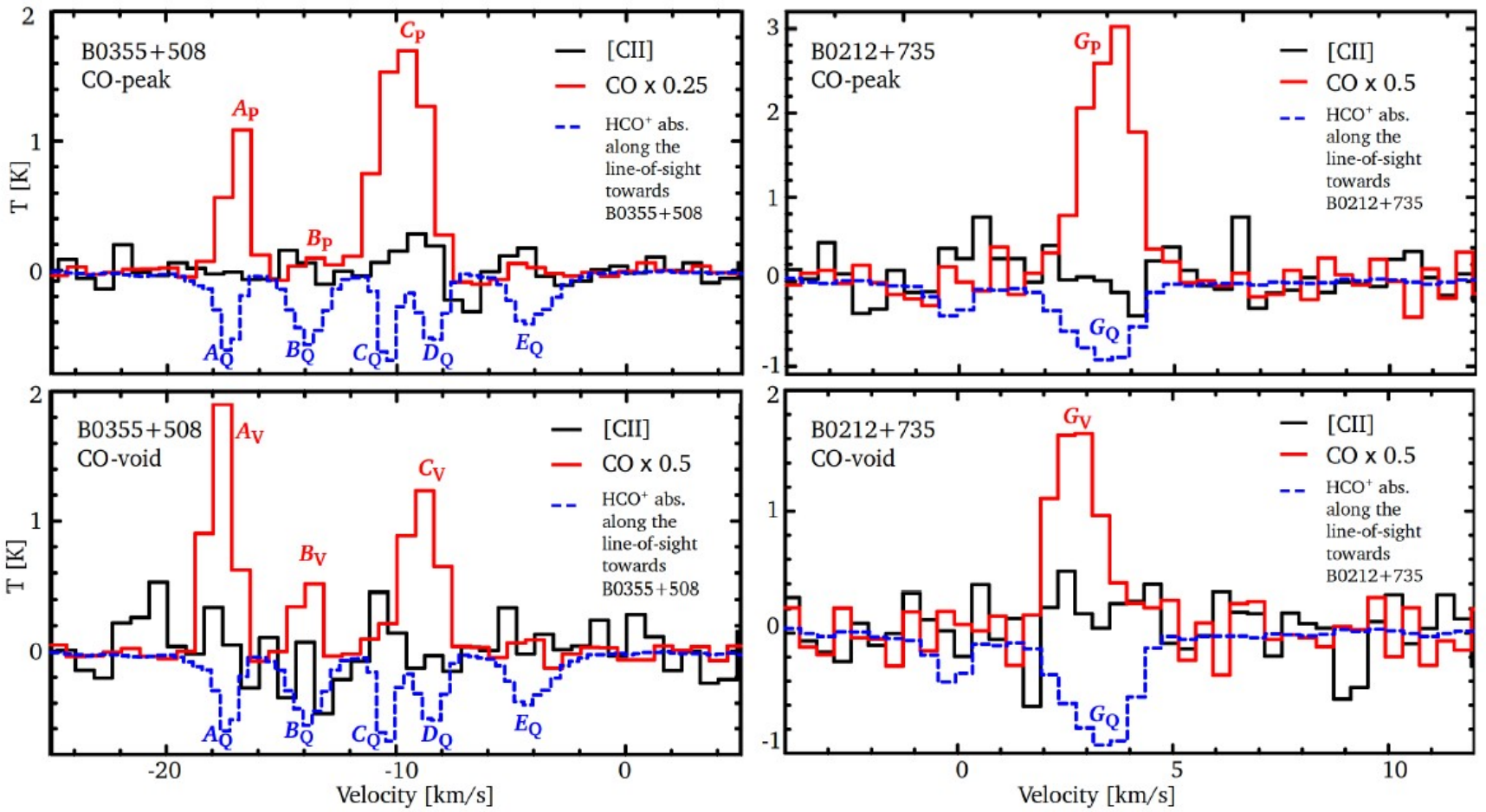

Fig. 2. [C II] (black) and CO (red; Liszt & Pety 2012) spectra at the positions CO-peak and CO-void in B0355+508 (left) and B0212+735 (right). The spectra of B0355+508 are smoothed to a velocity resolution of Δv=0.8 km/s; B0212+735 spectra are smoothed to Δv=0.4 km/s. The blue dashed line shows the HCO^+ absorption spectra along the lines of sight towards the quasars B0355+508 and 0212+735 (Liszt & Lucas 1996, 2000). The red letters mark CO velocity components in the CO-peak and the CO-void, blue letters mark HCO^+ absorption components along the line of sight towards the quasar. Identical capital letters mark related velocity components in the three positions. For better clarity we do not show the identified HCO^+ absorption component F_Q at v_{LSR}=2.5 km/s in B0212+735 (cf. Table 3) reported by Lucas & Liszt (1996).

note: multiple velocity components

observed intensities and upper limits for [CII]

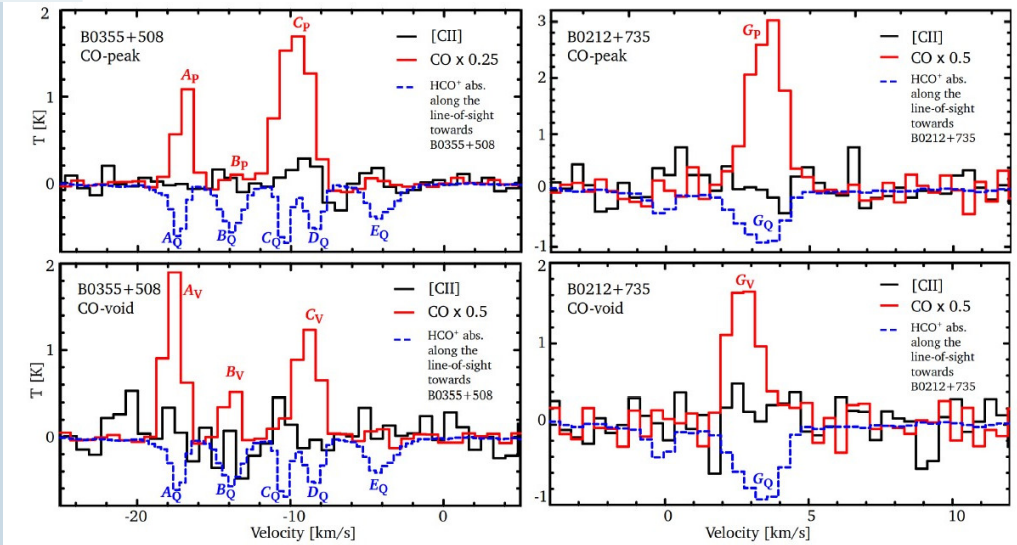

Table 2. Upper limits for the intensity compared to CO lines intensities of separated CO velocity components at the observed positions of the CO-peak and CO-void in B0355+508 and B0212+735.

(1)	(2) $v_{LSR\ CO}$ [km/s]	(3) Δv_{CO} [km/s]	(4) $I(CO)_{P/V}$ [K km/s]	(5) $I([C\,II])$ [K km/s]
B0212+735				
CO-peak				
A_P	-16.9 ± 0.1	2.4 ± 0.1	6.4 ± 0.7	<0.3
B_P	-13.8 ± 0.1	1.2 ± 0.4	1.1 ± 0.8	<0.3
C_P	-9.8 ± 0.1	1.2 ± 0.1	20.0 ± 2.0	<0.4
CO-void				
A_V	-17.6±0.1	1.1±0.1	5.2±0.6	<0.5
B_V	-13.8±0.1	1.1±0.1	1.8±0.3	<0.5
C_V	-8.9±0.1	1.9±0.1	4.9±0.5	<0.6
B0212+735				
CO-peak				
G_P	3.5±0.1	1.4±0.1	8.4±0.9	< 0.5
CO-void				
G_V	2.3±0.1	1.8±0.1	5.5±0.6	< 0.4

Notes. (1) Designation of the individual velocity components. The CO-peak and -void positions are marked by the subscripts P and V, respectively.
(2) v_{LSR} of the CO component(s) in the sources.
(3) Width of the CO line.
(4) Integrated CO line intensity in the positions CO-peak and CO-void, labelled by the footnotes P and V.
(5) Upper limits for the observed integrated [C II] intensity $I([C\,II])$. To estimate the upper limit of $I([C\,II])$ we assumed that the [C II] line is located at the same v_{LSR} as CO and that the [C II] line width is equal to Δv_{CO}.

- **break-down into identified velocity components**
  - some associated with CO
  - some only in HCO+ absorption

SOFIA/GREAT [CII] observations in nearby clouds near the lines of sight towards B0355+508 and B0212+735

Overview

- Science context
- Proposal
- Observations
- Interpretation and analysis
- Summary

- for comparison with predicted “diffuse cloud” [CII] intensities
  - H, H_2 column densities for individual velocity components from
    - CO intensities
      - line-of-sight towards quasar
      - CO peak
      - CO void
    - HCO^+ absorption along quasar l-o-s
    - HI 21 cm along quasar l-o-s
  - from this
    - total H column ($H+H_2$) from HCO^+, assuming appropriate fractionation
    - lower limit to total H column, from CO/H_2, ignoring HI
  - consistent with HI 21 cm columns

lower limits on H-column density from CO

total observed HI-21cm column density

Table 4. Molecular, neutral, and total hydrogen column densities and volume densities in the positions CO-peak, CO-void, and the LOS toward the quasars.

(1)	(2) $N(H_2)_{CO_Q}$ cm^{-2} 10^{20}	(3) $N(H_2)_{HCO^+}$ cm^{-2} 10^{20}	(4) $N(H)_{HCO^+}$ cm^{-2} 10^{21}	(5) $n(H)_{HCO^+}$ cm^{-3} 10^{3}	(6) $N(H_2)_{CO_P}$ cm^{-2} 10^{20}	(7) $N(H)_{CO_P}$ cm^{-2} 10^{21}	(8) $n(H)_{CO_P}$ cm^{-3} 10^{3}	(9) $N(H_2)_{CO_V}$ cm^{-2} 10^{20}	(10) $N(H)_{CO_V}$ cm^{-2} 10^{21}	(11) $n(H)_{CO_V}$ cm^{-3} 10^{3}	(12) $N(H\,I)_{tot}$ cm^{-2} 10^{20}
	LOS toward quasar					**CO-peak**			**CO-void**		
B0355+508											
A	10.4±1.1	4.3± 0.7	2.5±0.4	5.3±0.9	13.1±1.4	2.6±0.3	5.7±0.6	10.6±1.1	2.1±0.5	4.6±0.6	**62.8**
B	< 0.4±0.1	4.7 ±0.7	2.7±0.4	5.8±0.9	2.2±1.6	0.4±0.3	1.0±0.7	3.7±0.5	0.7±0.2	1.6±0.4	
C	31.2±3.1	4.7± 0.7	2.7±0.4	5.8±0.9	40.8±4.1	8.2±0.8	17.5±1.8	10.0±1.1	2.0±0.5	4.3±0.4	
D	<0.6±0.1	4.0± 0.7	2.3±0.4	4.9±0.9	–	–	–	–	–	–	
E	<0.8±0.1	4.3± 0.7	2.5±0.4	5.3±0.9	–	–	–	–	–	–	
B0212+735											
F	–	2.4 ± 0.4	1.4±0.2	1.5±0.2	–	–	–	–	–	–	**16.8**
G	22.5±4.8	10.8 ± 1.4	6.2±0.8	6.7±0.9	17.1±1.8	3.4±0.4	3.7±0.4	11.2±1.3	2.2±0.2	2.4±0.3	

Notes. Estimated molecular and total hydrogen column densities and volume densities along the line of sight towards the quasars and in the positions CO-peak and CO-void. The footnotes CO and HCO^+ note the underlying method used to derive these values. The CO-footnotes Q, P, V represent the positions LOS towards the quasar, CO-peak and CO-void.
(1) Designation of the assigned velocity components.
(2), (6), and (9) Molecular hydrogen column density derived from the CO emission by the use of Eq. 2. Liszt et al. (2010) give a $N(H_2)_{CO}$ of $N(H_2)_{CO} \approx 35\times10^{20}$ cm^{-2} for the LOS towards B0355+508. This value corresponds to the $N(H_2)_{CO}$ derived for component *C* along the line of sight towards B0355+508.
(3) Molecular hydrogen column density derived from the HCO^+ absorption along the line toward the quasar by the use of Eq. 1. The here calculated $N(H_2)_{HCO^+}$ for the components towards B0355+508 are consistent with the $N(H_2)_{HCO^+}$ given by Liszt et al. (2010) of $N(H_2)_{HCO^+} \approx 4.5\times10^{20}$ cm^{-2}.
(4) Total total hydrogen column derived from $N(H_2)_{HCO^+}$ and an assumed H_2 fraction of 35%; $N(H)_{HCO^+} = 5.7\times N(H_2)_{HCO^+}$
(7) and (10) Lower limits of the total hydrogen column density derived from the CO emission; $N(H)_{CO_{P/V}} = 2\times N(H_2)_{CO_{P/V}}$. The (unknown) contribution of H I to the total amount of hydrogen is not considered.
(5), (8) , and (11) volume hydrogen densities, derived by dividing $N(H)$ by the assumed cloud diameter d_C for an assumed cloud distance of 150 pc (d_C(B0355+508)=0.15 pc, d_C(B0212+735)=0.3 pc); $n(H)=N(H)/d_C$
(12) Total H I column density of the cold interstellar gas along the lines of sight towards the quasars. Form Dickey et al. (1983)

observed versus predicted

3σ upper limits

Table 2. Upper limits for the intensity compared to CO lines intensities of separated CO velocity components at the observed positions of the CO-peak and CO-void in B0355+508 and B0212+735.

(1)	(2) $v_{LSR\ CO}$ [km/s]	(3) Δv_{CO} [km/s]	(4) $I(CO)_{P/V}$ [K km/s]	(5) $I([C\,II])$ [K km/s]
B0355+508				
CO-peak				
A_P	-16.9 ± 0.1	2.4 ± 0.1	6.4 ± 0.7	<0.3
B_P	-13.8 ± 0.1	1.2 ± 0.4	1.1 ± 0.8	<0.3
C_P	-9.8 ± 0.1	1.2 ± 0.1	20.0 ± 2.0	<0.4
CO-void				
A_V	-17.6±0.1	1.1±0.1	5.2±0.6	<0.5
B_V	-13.8±0.1	1.1±0.1	1.8±0.3	<0.5
C_V	-8.9±0.1	1.9±0.1	4.9±0.5	<0.6
B0212+735				
CO-peak				
G_P	3.5±0.1	1.4±0.1	8.4±0.9	< 0.5
CO-void				
G_V	2.3±0.1	1.8±0.1	5.5±0.6	< 0.4

Notes. (1) Designation of the individual velocity components. The CO-peak and -void
positions are marked by the subscripts P and V, respectively.
(2) v_{LSR} of the CO component(s) in the sources.
(3) Width of the CO line.
(4) Integrated CO line intensity in the positions CO-peak and CO-void, labelled by the footnotes P and V.
(5) Upper limits for the observed integrated [C II] intensity $I([C\,II])$. To estimate the upper limit of $I([C\,II])$ we assumed that the [C II] line is located at the same v_{LSR} as CO and that the [C II] line width is equal to Δv_{CO}.

Table 5. Lower limits for the expected $I([C\,II])$ in diffuse clouds derived from the photo electric heating rate following Eq. 4.

(1)	(2) $I([C\,II])_{HCO^+}$ K km s^{-1}	(3) $I([C\,II])_{CO_P}$ K km s^{-1}	(4) $I([C\,II])_{CO_V}$ K km s^{-1}
LOS towards quasar	**CO-peak**	**CO-void**	
B0355+508			
A	1.4±0.2	1.5±0.2	1.2±0.1
B	1.5±0.2	0.3±0.2	0.4±0.1
C	1.5±0.2	4.7±0.5	1.1±0.1
D	1.3±0.2	–	–
E	1.4±0.2	–	–
B0212+735			
F	0.8±0.1	–	–
G	3.5±0.5	1.9±0.2	1.3±0.1

Notes. (1) Designation of the assigned velocity components.
2) Expected integrated [C II] intensity based on the total hydrogen column $N(H)_{HCO^+}$ derived from the HCO^+ absorptions and an H_2 fraction of 35%; (3)and (4) Expected integrated [C II] intensities in the positions CO-peak ($I([C\,II])_{CO_P}$) and CO-void ($I([C\,II])_{CO_V}$) based on molecular hydrogen column densities derived from the CO CO column density. The contribution of H I to the total amount of hydrogen is not considered.

a factor of 3 to 7 below expected!

- **diffuse cloud scenario rules out!**
- **[CII] excitation must be lower than in diffuse clouds**
  - **lower density (below critical density of [CII])**
    - **ruled out by cloud volume densities and cloud sizes**
  - **lower temperature?**

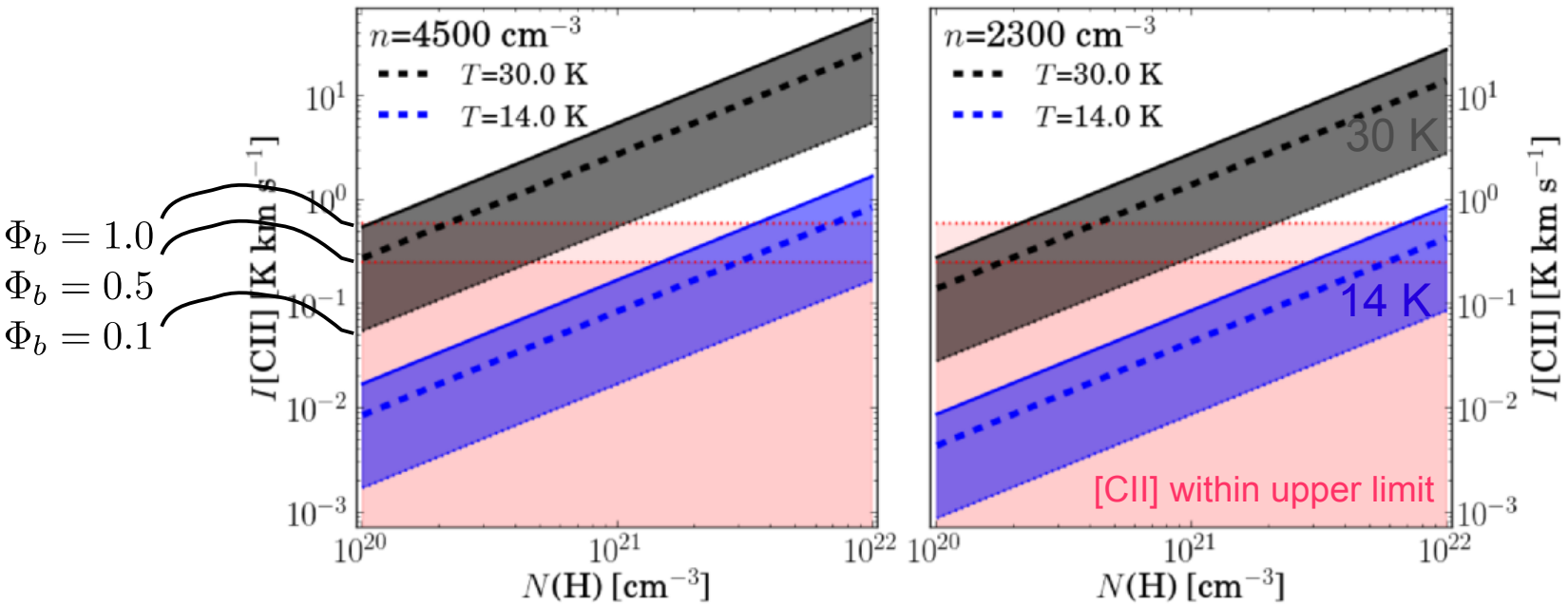

Fig. 3. Expected $I([\mathrm{C\,II}])$ for $n(\mathrm{H})$=4500 cm^{-3} (left) and $n(\mathrm{H})$= 2300 cm^{-3} (right) at different total hydrogen column densities $N(\mathrm{H})$ and temperatures calculated from Eq. 5. The filled grey areas show the expected $I([\mathrm{C\,II}])$ for a T=30 K. The blue areas show the expected $I([\mathrm{C\,II}])$ for a cold cloud with a kinetic gas temperature of 14 K, as indicated by the CO(2–1)/CO(1–0) ratio. The dashed lines (- - -) represent the $I([\mathrm{C\,II}])$ for a beam filling factor of Φ_b=0.5. The upper and lower edge of the grey and blue filled areas shows the $I([\mathrm{C\,II}])$ for a beam filling factor of Φ_b=1 and Φ_b=0.1, respectively. The red areas mark the upper limits of the [C II] observations.

simple analytical calculation:
consistent with observed column densities

→ need low temperature and/or lower column density for [CII] emitting gas

PDR-scenario (KOSMA-τ model)

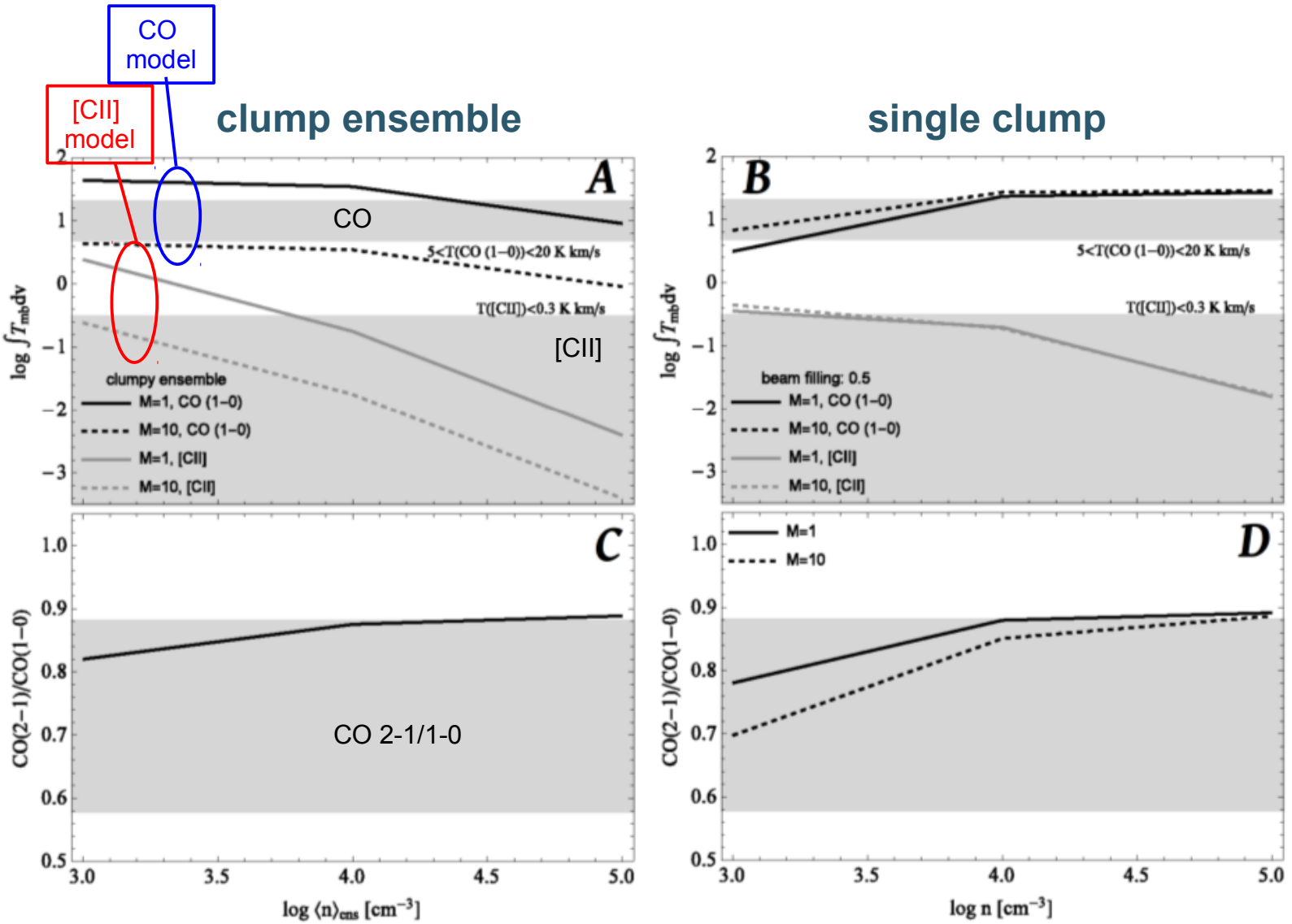

Fig. 4. PDR modelling (KOMSA-τ model; Röllig et al. 2006) of clumps with masses of M=1 and 10 $M_\odot$ for surface volume hydrogen densities of n(H)=10^3 to 10^5 cm^{-3}. The images on the left (*A* and *C*) illustrate the modelling for an ensemble of clumps. The images on the right (*B* and *D*) show the modelling for a single clump. For the single clump we anticipated a beam filling factor of Φ_b=0.5.
The images at the top (*A* and *B*) show the modelled [C II] and ^{12}CO(1–0) integrated line intensities. The black and grey lines show the modelled integrated line intensities of CO(1–0) and [C II]. The style of the line marks the anticipated clump mass. The grey areas show the rough lower and/or upper limits of the CO(1–0) and [C II] observations.
The images at the bottom (*C* and *D*) illustrate the modelled CO(2–1)/CO(1–0) ratio for clumps with M=1 and 10 $M_\odot$. The range of the observed CO(2–1)/CO(1–0) ratio (≃0.73±0.16) is marked by the grey area.

Jürgen Stutzki, Universität zu Köln

PDR scenario

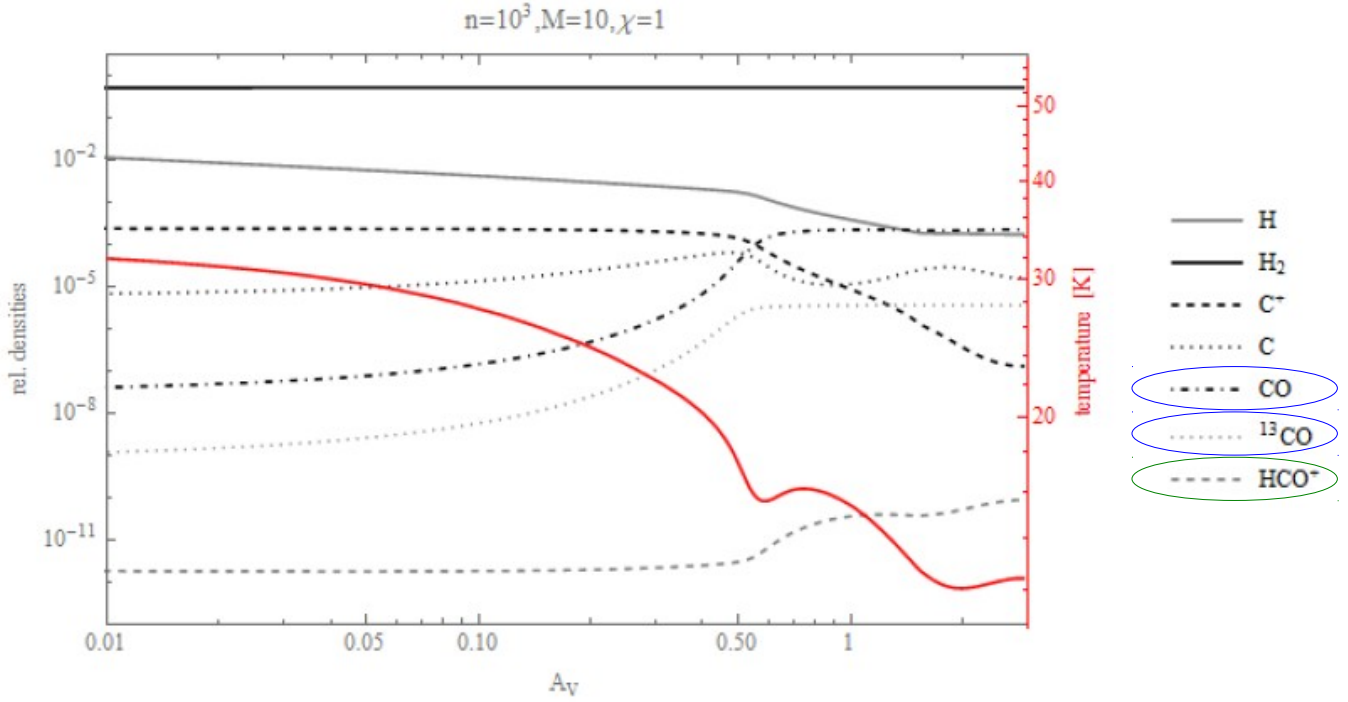

Fig. 5. Chemical profile of a clump with a surface volume hydrogen densities of $n(\mathrm{H})=10^3$ cm^{-3} and a mass of 10 $M_\odot$ penetrated by a standard Drain field of $\chi=1$. The relative densities of H^0, H_2, C^+, C^0, $^{12/13}CO$, and HCO^+ as function of A_V are shown by the black/grey lines (left axis). The temperature profile within the clump is shown by the red line (right axis).

- **HCO^+ consistent**
- **observed $^{12}CO/^{13}CO$ ratio requires small (<1 M_o) clumps or a clump ensemble**

Summary

SOFIA's New Zealand campaign, Christchurch airport, Summer 2013

- non-detection of [CII] 158 µm contradicts scenario of warm, non-LTE, diffuse clouds with sub-thermally excited CO
- non-detection implies less excited [CII]
  - lower densities contradict measured volume density and cloud size
  - lower temperatures (supported by CO intensities interpreted in thermalized case) constrain the cloud densities to below 2-5x10^3 cm^{-3} and [CII] emitting columns of below A_V=1
- the observed ^{12}CO and ^{13}CO J=2-1 and 1-0 intensities and the upper limit for [CII] are consistent with a clumpy cloud PDR scenario at G_0=1, 1-10 M_o clumps